

Photoacoustic Depth-Resolved Analysis of Tissue Models

A. BEENEN, G. SPANNER, and R. NIESSNER*

Institute of Hydrochemistry, Technical University of Munich, Marchioninstr. 17, D-81377 Munich, Germany

Pulsed photoacoustic laser spectroscopy was used for depth-resolved analysis of artificial tissue models. The technique was applied to investigate the spatial resolution capabilities of a fiber-optical-coupled photoacoustic sensor head. The time-resolved measurements confirmed the theoretical predictions of a depth resolution of 0.1 mm. In an adapted skin model, a strongly absorbing target could be detected up to a layer depth of 14 mm. At a layer depth of 5 mm, a lateral resolution of 3.5 mm was achieved. Because of the depth-resolving capability, this method is well suited as a complementary approach for two-dimensional imaging techniques.

Index Headings: Pulsed photoacoustic spectroscopy; Tissue model; Fiber optic; Depth resolution; Depth profile; Lateral resolution; Dye laser; Imaging.

INTRODUCTION

Medical techniques like X-rays, nuclear magnetic resonance (NMR), and scintigraphy have been developed to provide images of the inside of the human body without the need for invasive surgical operations. However, this capability does not mean that these techniques avoid all damage to the patient's body. X-rays, because of their carcinogenic nature, have been especially criticized. Scintigraphy, which is often used to examine organs and blood vessels, requires exposure to a considerable amount of radioactive radiation. Even the high magnetostatic fields applied in NMR have been suspected of having damaging effects on the human body, although no scientific evidence has been found up to now. Therefore, looking for new imaging techniques that enlarge or complement the abilities of current techniques seems to be recommended.

Optical methods appear to be suitable for this purpose. The determination of the oxygen saturation in the blood by optical transmission measurements is already a well-established technique. Photoacoustic spectroscopy (PAS) is a noninvasive optical method that exhibits many advantages in measuring spectral characteristics of strongly scattering samples like biological tissues. In contrast to transmission measurements, it is possible to determine the absorption coefficient independently of the scattering properties of the material. A special advantage of PAS is that, by measuring the time delay of the acoustic signal, one can obtain a depth profile of the material. For a new scanning technique that is able to provide both laterally resolved and depth-resolved images at least of layers in or close to the skin surface, PAS seems to be a promising method. Up to now PAS has been mainly applied to trace gas monitoring^{1,2} and depth-profiling studies of semiconductors,³ but there are already developments in the area of photoacoustic determination of blood contents.⁴ The main advantage of an imaging technique based on pulsed

PAS is that, by varying the wavelength of the incident light, one can perform spatially resolved spectroscopy.

THEORY

Sound Excitation by Laser Pulses. The pulsed photoacoustic effect consists of sound generation due to absorption of laser light. For effective excitation of photoacoustic pulses, an excimer-pumped dye laser can be used. If the space and time distribution of the light pulse is assumed to be Gaussian, an analytical expression for the pulse shape can be calculated.^{5,6} The resulting time-dependent pressure amplitude is shown in Fig. 1. The half-width of the compression part of the wave is given by the time τ_a which the acoustic wave takes to transverse the volume illuminated by the laser beam. The parameter τ_a is given by

$$\tau_a = \frac{2R}{v_s} \quad (1)$$

where v_s is the speed of sound in the medium, and R is the radius of the illuminated volume.

For biomedical samples with a high water content, $v_s = 1.5 \cdot 10^3$ m/s can be assumed. With a laser beam radius of several millimeters, the acoustic transverse time can be calculated to $\tau_a = 1$ to $10 \mu\text{s}$. The transverse time τ_a is identical to the half-width of the first compression pulse of the acoustic signal.

With pulsed laser sources, depth resolution can be obtained by using the time delay between the laser shot and the arrival of the acoustic pulse at the surface of the sample. The depth d of an absorbing object in a sample can be calculated as

$$d = v_s(\Delta t - t_0) \quad (2)$$

where Δt is the time delay between the arrival of the acoustic signal at the detector and the laser pulse. The actual v_s observed response time of the experimental setup originates from several parameters like the trigger-delay time of the photoacoustic system (see Experimental section).

With the use of a boxcar integrator, the position of the pulse maximum can be determined within one tenth of the half-width of the photoacoustic pulse.⁷ The theoretical detection limit of the depth resolution is therefore $\delta x \approx 0.1$ mm.

MATERIALS AND METHODS

Experimental. The experimental setup is shown in Fig. 2. The light from an excimer-pumped dye laser (Lambda Physik GmbH, Germany) is directed into an optical fiber (5 m, core diameter 1000 μm , Quartz & Silice PCS 1000B, France). With Coumarin 153 as the laser dye, the wavelength can be adjusted between 520

Received 7 March 1996; accepted 23 June 1996.

* Author to whom correspondence should be sent.

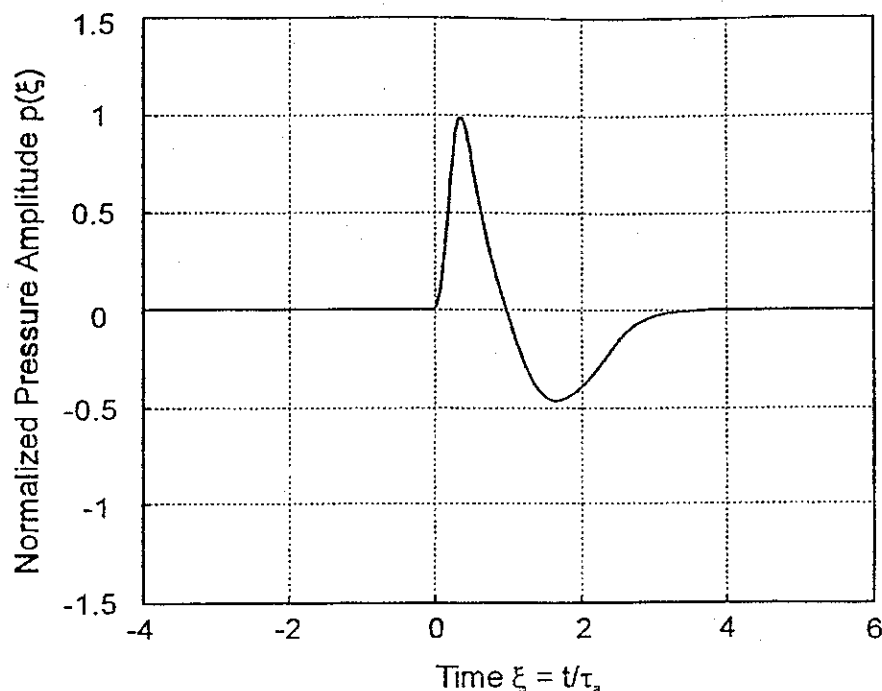


FIG. 1. Resulting time-dependent pressure amplitude.

and 600 nm. The pulse width of the laser beam is 10 ns. The pulsed laser light is guided through the optical fiber, and the output is focused on the sample. Because of absorption in the sample, an acoustic shock wave is generated. In the piezoelectric sensor head, this shock wave induces an electric signal. The signal is preamplified (gain 10) and then recorded by a boxcar system (Model 4400, EG&G Princeton Applied Research, U.S.A.). The function generator triggers the dye laser and at the same time supplies the reference trigger for the boxcar system.

Figure 3 shows the sensor head schematically. The sensor head consists of a compact aluminum housing in which the focusing lenses are integrated. A piezoelectric ring (PTZ 5A, diameter 10 mm, hole diameter 4 mm, thickness 2 mm, PI-Ceramic GmbH, Germany) is used for acoustic detection. The material of the sound detection plate is copper, and electric contact of the PZT is made with conducting silver-filled adhesive.

The laser light from the quartz fiber has a half-angle of 23.5° .⁸ As the amplitude of the photoacoustic signal is

inversely proportional to the square root of the beam radius,⁷ focusing of the laser beam is necessary. The focusing optics consist of two lenses. The first one serves as a collimator, and the second focuses the light onto the sample. By changing the distance between the second lens and the sample, it is possible to adjust the focus.

Because any piezoelectric material shows a pyroelectric effect, a conical light guide with a reflective coating was used to prevent stray light from heating the ceramic ring and thus producing unwanted signals. For the same reason the sound detection plate also has a reflective coating.

The small signal amplitudes (a few millivolts) require that all electrical cables and even the piezo ceramic itself be shielded against electromagnetic radiation. Since only

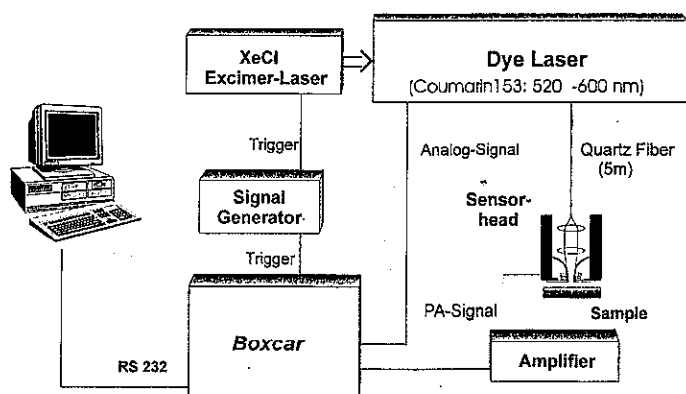


FIG. 2. Experimental setup.

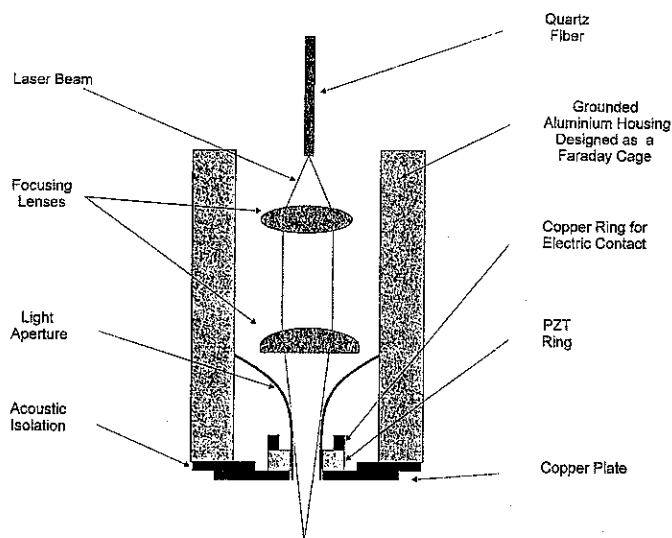


FIG. 3. Photoacoustic sensor head.

TABLE I. Acoustical properties of water and human skin/connective tissue.^a

	Speed of sound (m/s)	Impedance [10 ⁶ kg/(m ² s)]	Sound attenu- ation coeffi- cient (at 5 MHz) (dB/cm)
Water	1500	1.50	0.30
Skin and connective tissue	1460–1615	1.35–1.68	0.31

^a P. N. T. Wells, *Ultrasonics in Clinical Diagnostics* (Churchill Livingstone, London/New York, 1977).

a small hole in the detection plate (diameter 5 mm) lets the laser beam pass, the grounded aluminum housing with the copper plate in front serves as a high-frequency Faraday cage.

Tissue Model. For the investigation of the depth and lateral resolution possibilities of PAS in biological materials, it is necessary to find an appropriate tissue model. Emphasis should be placed on realistic modeling of the optical and acoustical properties of the different kinds of tissues. Especially the optical scattering coefficient, the absorption coefficient, and the scattering phase function have to match the corresponding values in tissue.

Cell culture tissues did not prove useful, because of their elaborate production, their limited layer thickness,⁹ and their general sensitivity to all kinds of environmental influences (e.g., temperature, sterility). Not only should the model be easy to set up and handle, but parameters such as thickness and scattering coefficient should be able to be changed easily. As is the case for tissue, the main ingredient of the model system should be water. To get an appropriate consistency, one can add gelatine.

Acoustical Properties. The most important acoustical parameters are velocity of sound, impedance, and attenuation. Human tissue consists of approximately 70–95% water, making the acoustical properties of tissue similar to those of water. A comparison of the acoustical parameters is shown in Table I.

Optical Properties. The optical properties of biological tissue are determined by the optical parameters μ_a , μ_s , and $S(\theta)$.¹⁰ The coefficients, μ_a and μ_s , represent the probabilities per unit pathlength that a photon will be absorbed or scattered, respectively. The total attenuation coefficient, μ_t , is the sum of the absorption and the scattering coefficients. The scattering phase function, $S(\theta)$, describes the angular dependence of the scattering, where the integral of $S(\theta)$ over 4π sr is unity. A useful simplifying parameter is the mean cosine of scattering angle g :

$$g = \int_{-1}^1 S(\theta) \cos \theta d(\cos \theta) \quad (3)$$

or the anisotropy parameter, g . Here $g = 0$ represents isotropic scattering, while $0 < g \leq 1$ represents forward scattering.¹¹

In tissues the dominant contribution to the total attenuation coefficient, μ_t , is the scattering coefficient, μ_s (cf. Table II). Therefore, only weakly absorbing material has to be taken into account in order to find a suitable model system. The optical parameters of aqueous suspensions

TABLE II. Reported optical parameters of tissue.

	Wave- length λ (nm)	Scatter- ing coef- ficient μ_s (1/cm)	Absorp- tion coef- ficient μ_a (1/cm)	Anisotropy parameter g
Skin	635	244 ^a	1.8 ^a	0.81 ^b
Muscle	515	530 ^a	11.2 ^a	Not measured
Lung	635	324 ^a	8.1 ^a	0.75 ^a

^a R. Marchesini, A. Bertoni, S. Andreola, and E. Melloni, *Appl. Opt.* **28**, 2318 (1989).

^b S. L. Jacques, C. A. Alter, and S. A. Prahl, *Laser Life Sci.* **1**, 309 (1987).

of milk powder (instant whole milk powder) and caolinit (known size distribution: for 49% of weight the diameter is $d < 2 \mu\text{m}$, for 34% d is between 2 and $6.3 \mu\text{m}$, and for 12.5% d is between 6.3 and $20 \mu\text{m}$) were measured to find a suitable tissue model. Suspensions of both materials were measured in different concentrations.

The total attenuation coefficient, μ_t , and the scattering phase function, $S(\theta)$, were measured with the narrow-beam experiment and the angle-dependent scattering measurement according to Flock et al.¹² To check the measurement techniques, we also measured polystyrene microspheres (No. C-106/C-107, Interfacial Dynamics Corporation, U.S.A.) of known, uniform size and refractive index. For this suspension, the values, μ_t , and the phase function, $S(\theta)$, can be calculated theoretically from the Mie scattering theory.¹³ The measured and calculated values agreed very well. The data from the measurements are presented in Table III. Table II shows the optical parameters of some tissues taken from the literature. Skin is probably the most interesting tissue for a possible medical application of photoacoustic spectroscopy. The total attenuation coefficient, μ_t , is proportional to the concentration of the added material (milk powder or caolinit, respectively). Therefore, a range of values can be easily achieved by simply varying the concentration. The scattering phase function represented by the anisotropy parameter, g , shows that milk powder comes very close to the optical properties of various kinds of tissues.

Hence, an appropriate skin model that agrees with skin in the optical and acoustical properties is an aqueous suspension of milk powder (62 g/L) and gelatine (35 g/L). This material can be produced with any required layer thickness.

DEPTH AND LATERAL RESOLUTION MEASUREMENTS

Investigation of the Depth Resolution. In the absorption layer, a photoacoustic signal is generated. With the measurement of the time difference between the trigger

TABLE III. Optical parameter of model components.

	Total attenuation coefficient with a concentration 1 g/L μ_t (1/mm)	Anisotropy parameter g
Caolinit	0.52	0.60 ± 0.015
Milk powder	0.39	0.79 ± 0.012

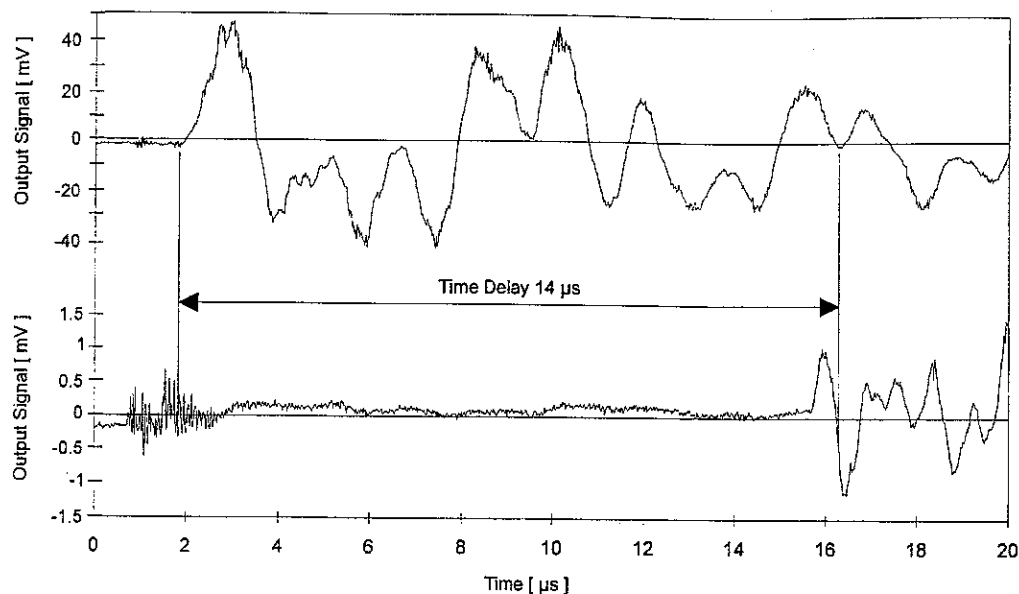


FIG. 4. Dependence of the time delay on the layer depth.

pulse and the detection of the pressure wave, the distance of the absorption layer from the detector can be determined.

Figure 4 shows two photoacoustic signals from different layer thicknesses. The upper curve shows the signal of a black absorber, which was placed directly on the detector surface, corresponding to a layer thickness of zero. The photoacoustic signal was observed after a time delay of 2.0 μs —a delay which is due to the pulse build-up time of the laser system after the triggering signal. The noise signal after 1 μs originates from the electromagnetic radiation of the excimer laser. The curve below

shows the photoacoustic signal of a black absorber, which is under a 22-mm gelatine layer (35 g/L). The signal starts after 16 μs . Again this number has to be corrected for the delay time of the laser system. It took the signal 14 μs to reach the sensor. With the speed of sound in gelatine (1560 m/s) and the use of Eq. 2, we get a layer thickness of 21.8 mm. This is the method used for all depth measurements reported here.

Measurements Using the Skin Model. For a strongly scattering medium it is more difficult to detect the position of the absorber because the signals are much weaker. For these kinds of measurements, a skin model was pro-

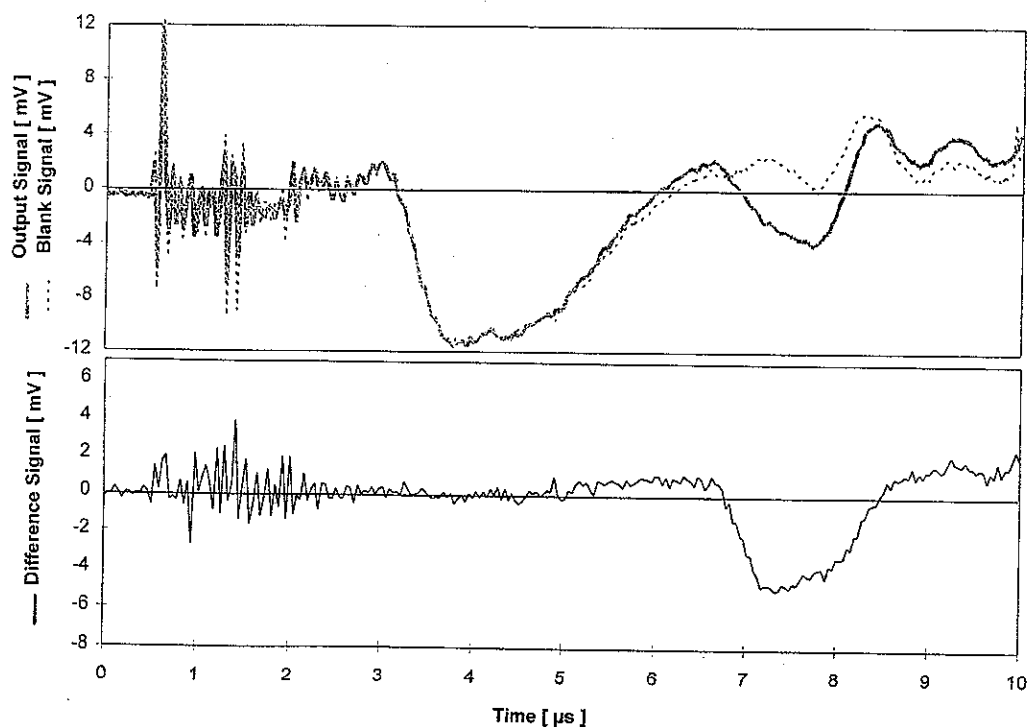


FIG. 5. Photoacoustic signal of a black absorber under a 8.5-mm layer of the skin model.

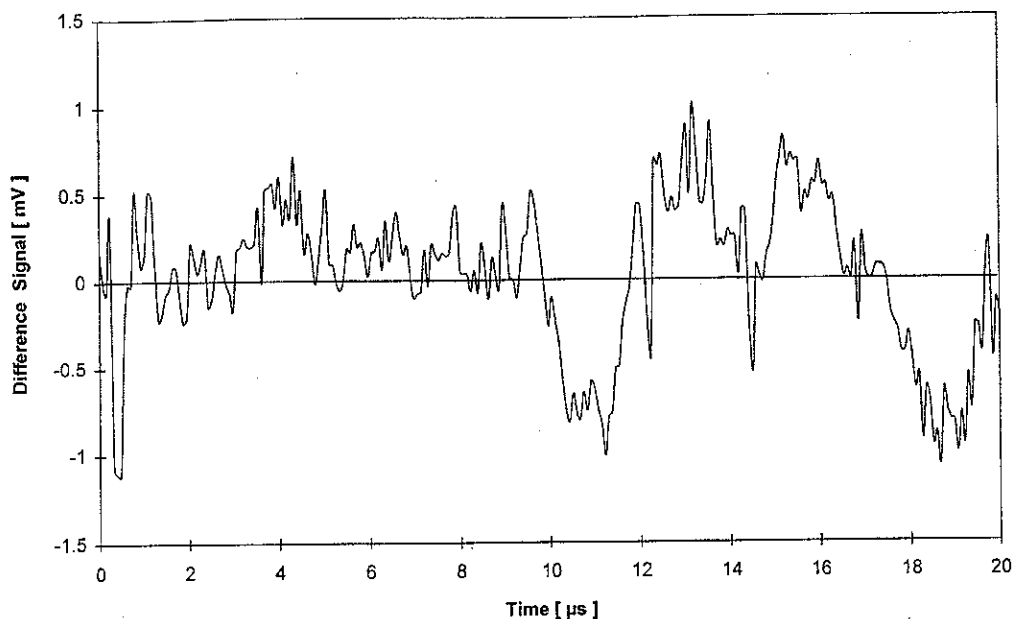


FIG. 6. Photoacoustic signal of a black absorber under a 12.9-mm layer of the skin model.

duced according to the description in the previous section.

Figure 5 shows a measurement of a black absorber beneath an 8.5-mm layer of the skin model. The upper continuous curve shows the initial photoacoustic signal. The existence of an absorbing layer at an 8.5-mm depth is not evident. The dashed line in the upper graph is the photoacoustic signal of the same sample without the black absorber. If the difference between the two signals is calculated by subtraction, the lower graph is obtained. In this graph a clear signal from the absorber appears after 6.5 μ s, indicating the layer thickness. The considerable background starting after 3 μ s in which the signal

is hidden originates from the absorption of scattered photons at the detection plate and in the medium.

In deeper layers the photoacoustic signal becomes weaker because of light scattering and finally disappears at a layer thickness of 14 mm. Figure 6 shows the difference signal, calculated as before, of a black absorber under a 12.9-mm-thick skin model layer. Here, the beginning of the signal after 9.7 μ s is no longer clearly visible.

Twenty different samples were prepared and measured. The results are summarized in Fig. 7. The accuracy of the thickness measurements by the time delay of the photoacoustic signal can be estimated with $dx = c \cdot dt$

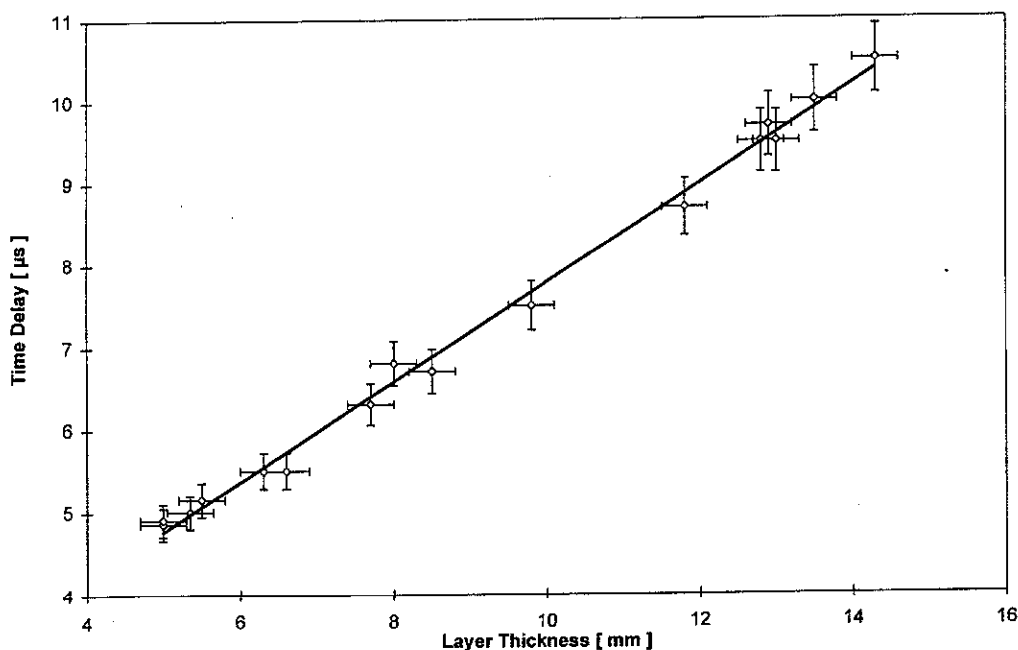


FIG. 7. Dependence of the time delay from different layer thicknesses.

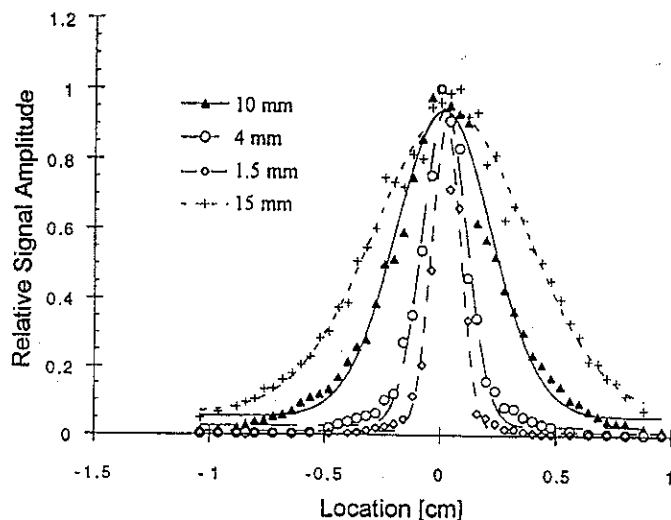


FIG. 8. Intensity distribution of the light along the beam diameter.

(Eq. 2) to be 0.15 mm, where Δt denotes the error of the determination of the delay time.

Lateral Resolution. The photoacoustic signal is excited in those parts of the sample in which the light is absorbed. For lateral resolution, focusing of the laser beam is important. In a scattering sample though, even the strongly collimated laser beam expands very quickly to a diffuse beam cone. To estimate the lateral resolution, we measured the beam diameter as a function of the layer thickness.

Scattering Radius at Different Layer Depths. For the determination of the scattering radius, samples with 10 g caolin/L water were produced. In this mixture the sample has a scattering coefficient of $\mu_s = 5.2 \text{ mm}^{-1}$. The intensity was measured along the diameter of the expanded laser beam with a photodiode which was moved in steps of 1 mm. The signal of the photodiode due to the laser pulses was measured as a function of time, and the maximum of the amplitude was taken. Figure 8 shows the intensity distribution of the light along the beam di-

ameter after the light has passed layers of different thickness. It is striking that after the light has passed through a thin layer, the expansion of the light cones is considerable.

Lateral Resolution by Photoacoustic Measurements. To get an idea of the imaging capabilities of PAS, we took a one-dimensional "picture" of the edge of a black absorber below a 5-mm layer of the skin model. The sample was mounted on an x-stage and moved in steps of 1 mm, while the sensor head was scanned across the edge of the black absorber. At each point the photoacoustic signal was measured. For optimal lateral resolution, the focus was adjusted to the surface of the absorber. Figure 9 shows the signal amplitudes as a function of the lateral position. The lateral resolution can be defined according to the Rayleigh criterion (full width at half-maximum). In this case the result is a full width of 7 mm.

The lateral resolution strongly depends on the diameter of the scanning laser beam and decreases with increasing depth due to the scattering in the medium. In samples with scattering properties similar to those of skin, imaging with a reasonable resolution will be possible only in layers very close to the surface.

CONCLUSION

Pulsed photoacoustic laser spectroscopy was used for depth-resolved and laterally resolved analysis of artificial tissue models. It turned out that a suspension of milk powder and water simulates the optical properties of human skin in a nearly optimal way. This model is uncomplicated to handle, and parameters like layer thickness and scattering coefficient can be easily adjusted.

Time-resolved measurements on this tissue model showed that a black absorber can be detected up to a layer depth of 14 mm. The accuracy of the thickness measurements by the time delay of the photoacoustic signal was 0.15 mm. With a layer depth of 5 mm, a lateral resolution of 3.5 mm was achieved. The limiting factor for the lateral resolution is strong light scattering in the sample.

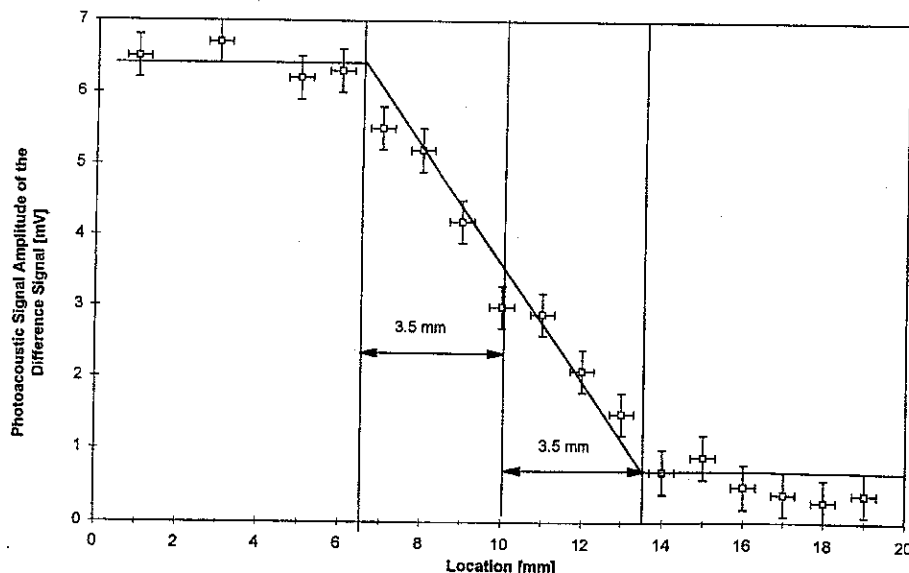


FIG. 9. PAS signal amplitudes in dependence of the lateral position.

The results presented here confirmed that it is possible to examine the human body at or underneath the surface by PAS techniques. Spectroscopic and depth-resolved measurements will be possible, but laterally resolved measurements do not appear to be practical.

1. M. W. Sigrist, *Analyst* **119**, 525 (1994).
2. M. W. Sigrist, S. Bernegger, and P. L. Meyer, *Infrared Phys.* **29**(2-4), 805 (1988).
3. A. C. Tam and Y. H. Wong, *Appl. Phys. Lett.* **36**, 471 (1979).
4. G. Spanner and R. Nießner, *AMI* **1**, 208 (1994).
5. S. A. Akhmanov, V. E. Gusev, and A. A. Karabutov, *Infrared Phys.* **29**(2-4), 815 (1989).
6. A. F. McDonald, *Appl. Phys. Lett.* **54**, 1504 (1989).
7. C. K. N. Patel and A. C. Tam, *Rev. Mod. Phys.* **53**, 518 (1981).
8. A. B. Sharama, S. J. Halme, and M. M. Butusov, *Optical Fiber Systems and Their Components* (Springer Verlag, New York, 1981).
9. T. Lindl and J. Bäuer, *Zell- und Gewebekulturen* (Gustav Fischer Verlag, Stuttgart, 1987).
10. R. R. Anderson, B. S. Parrish, and J. A. Parrish, *J. Invest. Dermatol.* **77**(1), 13 (1981).
11. C. F. Bohren and D. R. Huffman, *Absorption and Scattering of Light by Small Particles* (Wiley, New York, 1983).
12. S. T. Flock, B. C. Wilson, and M. S. Patterson, *Med. Phys.* **14**, 835 (1987).
13. H. C. Van De Hulst, *Light Scattering by Small Particles* (Wiley, New York, 1981).